



Universiteit
Leiden
The Netherlands

Signalling pathways that control development and antibiotic production in streptomyces

Urem, M.; Urem M.

Citation

Urem, M. (2017, October 10). *Signalling pathways that control development and antibiotic production in streptomyces*. Retrieved from <https://hdl.handle.net/1887/53237>

Version: Not Applicable (or Unknown)

License: [Licence agreement concerning inclusion of doctoral thesis in the Institutional Repository of the University of Leiden](#)

Downloaded from: <https://hdl.handle.net/1887/53237>

Note: To cite this publication please use the final published version (if applicable).

Cover Page



Universiteit Leiden



The handle <http://hdl.handle.net/1887/53237> holds various files of this Leiden University dissertation.

Author: Urem, M.

Title: Signalling pathways that control development and antibiotic production in streptomyces

Issue Date: 2017-10-10

CHAPTER IV

SCO4393, A NOVEL ENZYME INVOLVED IN *N*-ACETYLGLUCOSAMINE METABOLISM

Mia Urem, Magda A. Świątek-Połatyńska, Patrick Voskamp,
Navraj S. Pannu and Gilles P. van Wezel

ABSTRACT

Streptomyces bacteria are a bountiful source of diverse secondary metabolites, including the majority of clinical antibiotics. However, many of the biosynthetic gene clusters (BGCs) for natural products are silent under laboratory conditions. Better understanding of the connection between primary and secondary metabolic pathways, and the regulatory networks controlling them is required to activate the expression of these cryptic BGCs. A well-studied example is the activation of antibiotic production by metabolites derived from *N*-acetylglucosamine (GlcNAc), which modulate the activity of the global antibiotic repressor DasR inside the cell. Here, we present the phosphosugar isomerase SCO4393 as a novel member of the GlcNAc metabolic pathway. Deletion of SCO4393 relieves toxicity of both glucosamine (GlcN) and GlcNAc to *S. coelicolor nagB* mutants. Crystal structures of SCO4393 and SCO4393 in complex with GlcNAc-6P and with a culture-derived ligand, have been determined. The structures revealed that SCO4393 is a dimer with two active sites located at the interface of the monomers. The ligand-bound structure along with the ligand-free structure showed tightening of the active site upon binding. ITC binding studies strongly suggest that GlcNAc-6P is a major candidate substrate. Since accumulation of GlcNAc-6P is not toxic to *S. coelicolor* cells, we propose that the substrate of SCO4393 is a related aminosugar.

INTRODUCTION

With the rise of multidrug resistance in pathogenic bacteria, it is becoming increasingly critical to find novel drug therapies (O'Neill, 2014; WHO, 2014). The soil-dwelling, mycelial bacteria of the *Streptomycetaceae* family are prolific producers of diverse secondary metabolites that include some two third of all known antibiotics as well as immunosuppressant and anticancer drugs (Barka *et al.*, 2016; Bérdy, 2005, Hopwood, 2007). Despite the large number of antibiotics known to be produced by these bacteria, genome sequencing revealed that they likely have a greater capacity for the production of secondary metabolites than previously believed (Bentley *et al.*, 2002; Ikeda *et al.*, 2003; Ohnishi *et al.*, 2008; Cruz-Morales *et al.*, 2013). Streptomyces have the biosynthetic potential to produce dozens of secondary metabolites but the biosynthetic gene clusters (BGC) that specify many of these molecules remain poorly expressed under routine growth conditions (Medema *et al.*, 2015; Nett *et al.*, 2009). Current strategies for the activation of BGCs include the exploitation of bacterial responses to environmental triggers, the manipulation of metabolic pathways and regulatory networks, as well as the application of elicitors, identified from the ecological backgrounds of streptomyces, during screenings (Okada & Seyedsayamdost, 2016; Rutledge & Challis, 2015; van der Meij *et al.*, 2017; Zhu *et al.*, 2014a).

In the model organism *Streptomyces coelicolor*, *N*-acetylglucosamine (GlcNAc) is a preferred source of carbon and nitrogen (Nothaft *et al.*, 2003a; Nothaft *et al.*, 2010). GlcNAc is abundantly available in its dimeric form, *N*-*N'*-diacetylchitobiose [(GlcNAc)₂], as a component of chitin. GlcNAc is also found in cell wall peptidoglycan (PG), the chains of which consist of alternating GlcNAc and *N*-acetylmuramic acid (MurNAc) residues cross-linked via peptide bridges. Under rich nutritional conditions (feast), GlcNAc activates growth and represses development and antibiotic production (Rigali *et al.*, 2006; Rigali *et al.*, 2008). Under poor growth conditions (famine), GlcNAc instead activates development and antibiotic production. This phenomenon has been exploited to elicit secondary metabolites on minimal media during screens for novel antibiotics (Zhu *et al.*, 2014b).

The activation of antibiotic production and developmental onset by GlcNAc under poor growth conditions is mediated via the GntR-family repressor DasR (Rigali *et al.*, 2006; Rigali *et al.*, 2008). This global nutrient sensory regulator controls the uptake and metabolism of GlcNAc via direct binding to the promoter regions of the *chi*, *nag* and *pts* genes, encoding the enzymes of the chitinolytic system, GlcNAc metabolism and the phosphoenolpyruvate-dependent phosphotransferase system (PTS), respectively (Świątek-Połatyńska *et al.*, 2015; Świątek *et al.*, 2012a). In *Streptomyces coelicolor*, DasR also directly controls all the pathway-specific regulators for antibiotic production and the regulators for iron-chelating siderophore production (Świątek-Połatyńska *et al.*; 2015, Craig *et al.*, 2012; Lambert *et al.*, 2014). The DNA-binding activity of DasR is modulated by intracellular metabolites, whereby GlcNAc metabolic intermediates GlcNAc-6P and GlcN-6P allosterically induce the release of DasR from its recognition sites (Tenconi *et al.*, 2015; Rigali *et al.*, 2008; Fillenberg *et al.*, 2015; Świątek-Połatyńska *et al.*, 2015).

Monomeric GlcNAc, *e.g.* released during autolytic degradation of the cell wall, is taken up by *S. coelicolor* via the PTS, thereby phosphorylating the incoming GlcNAc to GlcNAc-6P (Nothaft *et al.*, 2003a; Nothaft *et al.*, 2010). To metabolise GlcNAc from chitin, chitinolytic enzymes are secreted which produce (GlcNAc and its oligomers for internalization of via ABC-transporter complex DasABC-MsiK (Colson *et al.*, 2008; Saito *et al.*, 2007; Schrempf, 2001). After the intracellular cleavage of (GlcNAc)₂, monomers of GlcNAc are phosphorylated by *N*-acetylglucosamine kinase NagK (Świątek *et al.*, 2012a). Following

from GlcNAc-6P, deacetylation by NagA forms glucosamine 6-phosphate (GlcN-6P) which is a central molecule at the intersection of multiple metabolic pathways, including glycolysis via conversion to fructose 6-phosphate (Fru-6P) by glucosamine-6-phosphate deaminase NagB (Świątek *et al.*, 2012a).

GlcNAc and its deacetylated derivative glucosamine (GlcN), are toxic to *S. coelicolor* *nagB* mutants, presumably due to the accumulation of GlcN-6P or a derivative thereof (Świątek *et al.*, 2012b). Spontaneous suppressor mutations were obtained for *S. coelicolor* *nagB* mutants that circumvented the toxicity of GlcNAc and/or GlcN. Mutation of *nagA* surprisingly restored growth of *nagB* mutants on both GlcNAc and GlcN, which suggests that GlcN may be metabolised via the GlcNAc pathway (Świątek *et al.*, 2012b). Two novel aminosugar-related genes were discovered in this screen (Świątek, 2012; this thesis), namely the ROK-family regulatory gene SCO1447 (*rokL6*), mutation of which exclusively relieves toxicity of GlcN to *nagB* mutants, and SCO4393, which encodes a putative phosphosugar isomerase. Deletion of the latter restores the ability of *nagB* mutants to grow in the presence of either GlcN or GlcNAc.

SCO4393 is a highly-conserved protein among streptomycetes and is also found in various other bacteria. In this work, we provide a functional and structural analysis of SCO4393 of *S. coelicolor* and analyse its role in the metabolism of aminosugars GlcN and GlcNAc. Structural studies supported by *in vitro* binding assays provide the first hints into the potential ligand of this novel primary metabolic enzyme.

MATERIAL AND METHODS

BACTERIAL STRAINS, CULTURE CONDITIONS, PLASMIDS AND OLIGONUCLEOTIDES

All strains described in this work are listed in Table S1. *Escherichia coli* was grown and transformed according to standard procedures (Sambrook *et al.*, 1989) with *E. coli* JM109 serving as the host for routine cloning, and *E. coli* ET12567 (MacNeil *et al.*, 1992) for the isolation of non-methylated DNA for transformation into *Streptomyces* (Kieser *et al.*, 2000). For heterologous protein expression, *E. coli* Rosetta™(DE3)pLysS from Novagen was used. *E. coli* was grown in Luria-Bertani (LB) media in the presence of selective antibiotics as required, with the following final concentrations; ampicillin (100 µg/ml) and chloramphenicol (25 µg/ml).

Streptomyces coelicolor A(3)2 M145 was obtained from the John Innes Centre strain collection and was the parent of all mutants. *S. coelicolor* *nagA*, *nagB* and *nagK* mutants (Świątek *et al.*, 2012a) and *nagB* suppressor mutants (Świątek, 2012), have been described previously. All *Streptomyces* media and routine techniques, including transformation via protoplast regeneration, are described in the *Streptomyces* manual (Kieser *et al.*, 2000). A mixture of 1:1 yeast-extract malt extract (YEME) and tryptic soy broth (TSB) liquid media was used to cultivate mycelia for protoplast preparation, and glucose-containing R5 agar media, with appropriate selective antibiotics, was used for protoplast regeneration after transformation. SFM (soy flour mannitol) agar was used for the cultivation of spores. Phenotypic characterization was done on R5 and minimal media (MM) agar supplemented with sugars as stated and where appropriate with the antibiotics apramycin (50 µg/ml) and/or thiostrepton (20 µg/ml) as selective markers.

All plasmids and oligonucleotides described in this work are summarised in Tables S1 and S2 of the supplemental material, respectively. The shuttle vector pHJL401 was used as a low-copy plasmid in *Streptomyces* (Larson & Hershberger, 1986), which is very well suited for genetic complementation experiments (van Wezel *et al.*, 2000a). The unstable multi-copy shuttle vector pWHM3 (Vara *et al.*, 1989) was exploited for gene replacement strategies (van Wezel *et al.*, 2005). Cre recombinase expressing plasmid, pUWLcre (Fedoryshyn *et al.*, 2008) was used for the creation of deletion mutants via genetic excision via *loxP* marked sites (see below for details). Expression vector pET-15b (Novagen), which introduces an N-terminal His-Tag, was used for heterologous expression of SCO4393. All DNA sequencing was performed by BaseClear BV (Leiden, The Netherlands).

GENETIC COMPLEMENTATION AND KNOCK-OUT MUTANTS

For genetic complementation of SCO4393, its coding region and 217 bp upstream region, likely encompassing the promoter region, was amplified from *S. coelicolor* M145 genomic DNA using primers compF-217 and compR+762 (Table S2), and cloned into pHJL401 to give plasmid pGWS1051.

The procedure for the creation of *S. coelicolor* gene replacement and deletion mutants is described in detail in (Świątek *et al.*, 2012a). Gene replacement mutants were generated via homologous recombination, with the gene of interest replaced by the apramycin resistance cassette *aac(C)IV*. For this, the upstream and downstream flanking regions of SCO4393 were PCR-amplified from genomic DNA using primer pairs LF-1438/LR+15 and RF+768/RR+2157 and cloned into pWHM3 using engineered EcoRI/XbaI and XbaI/HindIII restriction sites, respectively. The apramycin resistance cassette flanked by *loxP* sites was cloned in-between as an XbaI fragment. The resulting knock-out plasmid was designated pGWS1052 and introduced into *S. coelicolor* via protoplast transformation. Correct recombination events were checked by the appropriate antibiotics resistance

and confirmed by PCR. To obtain deletion mutants, the apramycin resistance cassette was excised by introduction of Cre recombinase expressing plasmid, pUWLcre (Fedoryshyn *et al.*, 2008), which allows for efficient removal of the cassette via the loxP recognition sites (Khodakaramian *et al.*, 2006). Deletion mutants were checked based for the appropriate antibiotic sensitivity (loss of apramycin resistance) and confirmed by PCR.

HETEROLOGOUS EXPRESSION AND PURIFICATION OF SCO4393

For *in vitro* experiments and structure elucidation via X-ray crystallography, N-terminally His₆-tagged SCO4393 was expressed in *E. coli* Rosetta™(DE3)pLysS. SCO4393 was PCR amplified from *S. coelicolor* genomic DNA using primers pETF-1and pETR-756 (Table S2), and cloned into pET15b. His₆-tagged SCO4393 was purified using a Ni-NTA column (GE Healthcare) with Isolation Buffer (500 mM NaCl, 5% glycerol, 50 mM HEPES, 10 mM β-mercaptoethanol, pH 8) containing 250 mM imidazole, as described (Mahr *et al.*, 2000). Fractions containing SCO4393 were pooled and concentrated before further purification by size exclusion chromatography (Superdex 200) with Isolation Buffer. Fractions containing SCO4393 were pooled and concentrated prior to use in crystallization trials and *in vitro* experiments. Protein was concentrated using 10 kDa molecular weight cut-off centrifugal filter units (Amicon) and samples were analysed by 15% SDS-PAGE and native PAGE electrophoresis.

PROTEIN CRYSTALLIZATION CONDITIONS

Purified SCO4393 at a concentration of 15-20 mg/ml was used to screen crystallization conditions by sitting-drop vapour-diffusion using the PGA Screen (Molecular Dimensions), Clear Strategy Screens CSS-I and CSS-II (Molecular Dimensions), JCSG+ (Qiagen/Molecular Dimensions) and the PACT screen (Molecular Dimensions) as well as optimization screens at 20°C. The 75 μL reservoir of 96-well Innovaplate SD-2 plates was pipetted by a Genesis RS200 robot (Tecan) and drops were made by an Oryx6 robot (Douglas Instruments). SCO4393 crystals with the open-ring intermediate were obtained in 0.2 M MgCl₂, 0.1 M TRIS (pH 8.5) and 25% (w/v) PEG MME 2000. All other crystals were obtained from JCSG number 83 (96-well G11) which consisted of 2.0 M Ammonium sulphate, 0.1 M BIS-Tris, pH 5.5. Crystals were soaked in cryoprotectant solution (mother liquor with 10-20% glycerol) in the presence or absence of 100mM ligand candidates, and flash-frozen in liquid nitrogen.

TABLE 1. Data collection and refinement statistics (molecular replacement).

	Ligand	GlcNAc-6P	GlcN-6P
Data collection			
Space group	P 1 2 1 1	P 6 5 2 2	P 6 5 2 2
Cell dimensions			
<i>a</i> , <i>b</i> , <i>c</i> (Å)	60.91, 99.03, 73.45	88.06, 88.06, 283.46	87.57, 87.57, 273.21
α, β, γ (°)	90, 106.07, 90	90, 90, 120	90, 90, 120
Resolution (Å)*	1.95 (1.95 – 1.99)	2.52 (2.52 – 2.61)	1.64 (1.64-1.74)
<i>R</i> _{meas}	0.167 (1.115)	0.256 (2.918)	0.202 (1.461)
<i>I</i> / σ <i>I</i>	8.8 (1.7)	9.7 (1.2)	4.3 (0.1)
CC(1/2)	0.993 (0.596)	0.998 (0.527)	0.986 (0.387)
Completeness (%)	98.3 (81.4)	100.0 (100.0)	81.7 (19.2)
Multiplicity	5.3 (5.1)	18.9 (19.5)	4.4 (1.2)
Refinement			
Resolution (Å)	1.95	2.52	1.64
No. reflections	57 318	21 792	59 305
<i>R</i> _{work} / <i>R</i> _{free}	0.196 (0.317)/	0.208 (0.348)/	0.267 (0.469)/
	0.241 (0.343)	0.250 (0.402)	0.301 (0.550)
No. atoms	7617	3681	3580
R.m.s. deviations			
Bond lengths (Å)	0.014	0.012	0.018
Bond angles (°)	1.56	1.744	1.851

*Values in parentheses are for highest-resolution shell.

STRUCTURAL DATA COLLECTION

X-ray data were collected at the European Synchrotron Radiation Facility (Grenoble, France) on beamline ID-23 for SCO4393 with the open-ring intermediate: 1410 images were collected on a Pilatus 6M detector at an X-ray wavelength of 0.9724 Angstroms, an exposure time of 0.037 seconds, transmission of 10% and an oscillation range of 0.2 degrees., while uncomplexed SCO4393 and SCO4393 in complex with GlcNAc-6P were collected on beamline ID-29 with a Pilatus 6M detector. For the native/uncomplexed crystal, 1020 images were collected at 1.2727 Å wavelength with an exposure time of 0.02 seconds, transmission of 100% and an oscillation range of 0.05 degrees. For SCO4393/GlcNAc-6P crystals, 680 images were collected at 0.976251 Angstroms wavelength with an exposure time of 0.02 seconds, transmission of 47.34% and an oscillation range of 0.1 degrees, XDS (Kabsch, 2010) was used to process all the data collected while aimless (Evans & Murshudov, 2013) was used for scaling and merging the integrated intensities. Table 1 shows the data collection and refinement statistics for all data sets obtained.

STRUCTURE DETERMINATION, REFINEMENT AND ANALYSIS

The structure of SCO4393 with the open-ring intermediate was solved by molecular replacement with Molrep (Vagin & Teplyakov, 2000) using the structure of a putative phosphoheptose isomerase from *Bacillus halodurans* C-125 determined at the Joint Center for Structural Genomics (PDB code 3CVJ) as a search model. The other structures were solved by molecular replacement with Molrep, but using the refined SCO4393 structure with the open-ring intermediate as the starting model. All structures were iteratively refined with REFMAC5 (Murshudov *et al.*, 2011) from the CCP4 package (Winn *et al.*, 2011) and manual model building and adjustments were done with Coot (Emsley *et al.*, 2010). The quality of the final models was validated with Molprobit (Chen *et al.*, 2010) and wwPDB Validation Service (Berman *et al.*, 2003). The ligand molecules were validated by Privateer (Agirre *et al.*, 2015). Final refinement statistics for all structures are given in Table 1. All figures showing structural representations were prepared with the program PyMOL (The PyMOL Molecular Graphics System, Version 1.8 Schrödinger, LLC).

ISOTHERMAL TITRATION CALORIMETRY

In vitro analysis of SCO4393 interaction with potential ligand candidates was examined thermodynamically by isothermal titration calorimetry (ITC) using a VP-ITC microcalorimeter (Microcal). To minimise interference of salts and other buffer components during ITC experiments, the buffer SCO4393 was taken up with was exchanged with ITC Buffer (50 mM HEPES, pH 8) using 10 kDa molecular weight cut-off centrifugal filter unit (Amicon) until the NaCl concentration was reduced below 50 µM. Following this, SCO4393 was dialysed overnight in 1L of ITC Buffer at 4°C to further reduce the concentration of salt and glycerol. The buffer from the dialysis was used to prepare the ligand samples (1 mM) to minimise discrepancies with the SCO4393 samples. Ligand was titrated at 6 or 8 µl injections into the sample cell containing 50 mM SCO4393 at 25°C. Data analysis and graphic representation were done using the program Origin (Microcal).

BIOINFORMATICS ANALYSIS

Motifs were predicted using InterProScan (Zdobnov & Apweiler, 2001) and Pfam 24.0 (Finn *et al.*, 2008) and protein homology searches were performed using BLASTp (Altschul *et al.*, 2005). Synttax used for gene synteny (Oberto, 2013). Protein alignments were visualised using Boxshade (www.ch.embnet.org/software/box_form.html).

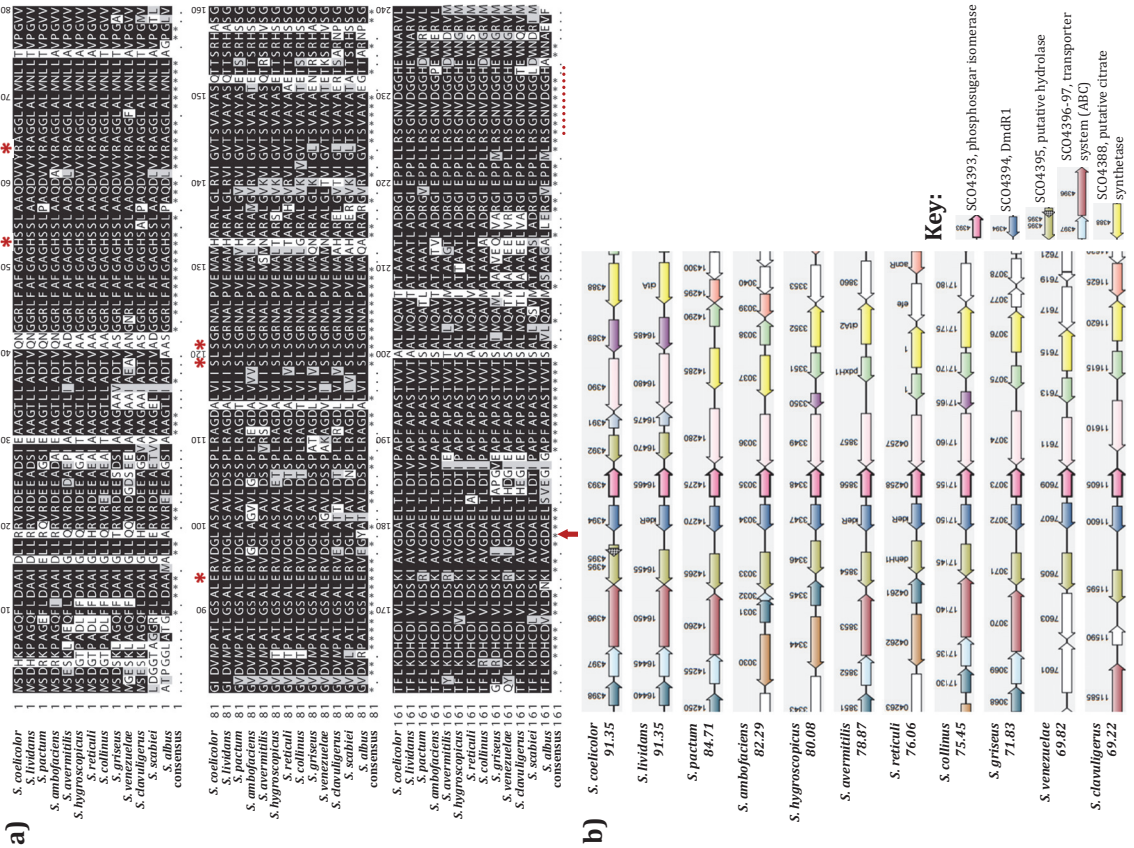
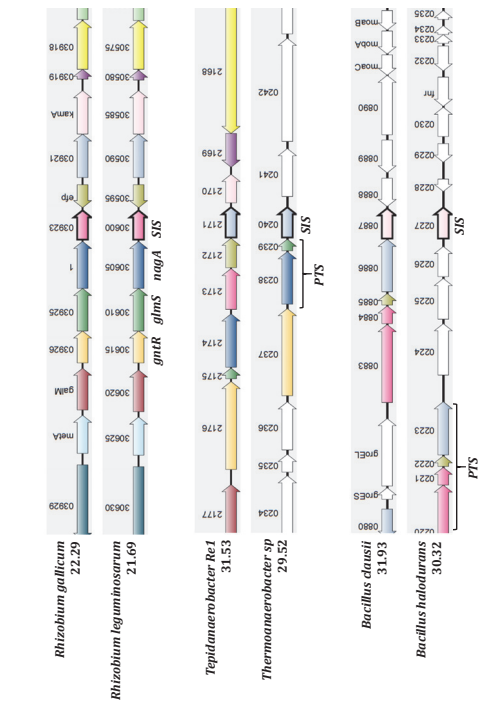


FIGURE 1. Sequence alignment and gene synteny for SCO4393.
 a) Alignment of the SCO4393 protein sequence with homologs from other *Streptomyces* species up to residue 240. Identical amino acids are shaded black, and amino acids with similar properties are in grey with a consensus of the alignment given below (*, identical; ·, similar). The D179N mutation identified in SMA11 is indicated with a red arrow (below). Residues likely to be important for ligand binding (see Fig. 4) are indicated with red stars (*, above) and the loop that conformationally shifts during ligand binding (see Fig. 5) is underlined by a red dotted line (below). The image was generated using Boxshade.
 b) Gene synteny between SCO4393 in *S. coelicolor* and homologs in other *Streptomyces* species. Analysis was done using Synttax (scores are given).
 c) Gene synteny of SCO4393 homologs found in some species of firmicutes and proteobacteria done using Synttax (scores are given). SCO4393 orthologs in *Rhizobium* species are located close to *nagA*, *glnS* and a gene for a GntR transcriptional regulator. In *Bacilli* and *Thermoanaerobacteria*, SCO4393 orthologs are located in proximity to genes of PTS components and other PTS-related genes. Homologs are presented in the same colours and highlighted in the key for *S. coelicolor*. Genes of interest in other bacteria are annotated and SCO4393 homologs are labelled 'SIS'.

c)



RESULTS

MUTATIONS IN SCO4393 RELIEVE TOXICITY OF AMINOSUGARS TO *S. COELICOLOR* *nagB* MUTANTS

Genomic analysis of suppressor mutants of the *S. coelicolor nagB* deletion mutant previously identified novel candidates in the metabolic pathways of GlcNAc and GlcN as well as the regulation thereof (Świątek, 2012; this thesis). One such mutation was identified in SCO4393 in suppressor mutant SMA11, which harboured a single nucleotide permutations (SNP) at nucleotide position 535 (G to A substitution), leading to a non-silent change from aspartic acid to asparagine (Asp179Asn) in the sugar isomerase (SIS) domain of the predicted gene product (Świątek, 2012). Other suppressor mutants were also screened for possible mutations in SCO4393 by introducing construct pGWS1051, which expresses wild-type SCO4393. Transformants regaining aminosugar sensitivity, as a result of the presence of wildtype copies of SCO4393 expressed from the plasmid, were confirmed by sequencing the PCR-amplified SCO4393 gene from a number of mutants. Indeed, suppressor SMA13 harboured the same G to A substitution at position 535 as SMA11 as well as a frameshift as a result of an insertion at nucleotide position 561. Together, this indicates that mutations in SCO4393 are sufficient to suppress the toxicity of GlcNAc (and GlcN) to *nagB* deletion mutants. This suggests that a functional SCO4393 protein is necessary for the toxic effect of the aminosugars and that the sugar isomerase likely plays a currently undefined role in the formation of the toxic intermediate.

SCO4393 IS A HIGHLY CONSERVED SIS-DOMAIN PROTEIN IN *STREPTOMYCES*

SCO4393 is a conserved hypothetical protein with a sugar isomerase (SIS) domain (Bateman, 1999), predicted to span almost the entire length of the protein. SIS domains are typically found in phosphosugar-binding proteins, including some with transcriptional control over the biosynthetic genes of phosphosugars, and phosphosugar isomerases such as MurQ and GlmS (Jaeger & Mayer, 2008; Reith & Mayer, 2011; Kim *et al.*, 2009). The closest paralogue of SCO4393 is MurQ (SCO4307) but the proteins only share 31% amino acid identity (43% positives). MurQ contains a SIS-esterase domain that is responsible for the conversion of MurNAc-6P to GlcNAc-6P by cleavage of the lactyl ether bond. This, in combination with the relatively low sequence similarity, suggests that no functional homologue of SCO4393 exists in *S. coelicolor*.

There is high sequence similarity (at least 80% aa identity and 90% positives) between the SCO4393 orthologues in different *Streptomyces* species (Fig. 1A). Gene synteny analysis shows that also the genomic region around SCO4393 is highly conserved among streptomycetes (Fig. 1B). The regulatory gene *dmdR1* (SCO4394) is expressed divergently from SCO4393 in *S. coelicolor* and many, but not all, other streptomycetes. DmdR1, which is a repressor of iron utilization and also controls production of iron-chelating siderophores, is induced by GlcNAc in *Streptomyces* via repression of DasR (Craig *et al.*, 2012). A DasR-responsive element (*dre*) has been identified in the intergenic region of SCO4393 and *dmdR1*, 54 nt upstream of the translational start of SCO4393 (Craig *et al.*, 2012). Other genes in the genomic region of SCO4393 with high gene synteny include a putative hydrolase, components of an ABC transporter and a putative citrate synthetase.

Based on gene synteny analysis, homologs of SCO4393 with an amino acid similarity of 30-40% (45-60% positives) and containing a SIS-domain of unknown function are present in several other bacterial phyla, including firmicutes and proteobacteria. In Gram-negative soil-dwelling Rhizobia, the orthologous gene is suggestively located downstream of the aminosugar-related metabolic genes *glmS* and *nagA*, with a gene encoding a GntR regulator

in the same operon (Fig. 1C). In firmicutes, such as *Thermoanaerobacter* and *Bacillus* species, SCO4393 homologs lie in close proximity to genes encoding components of the PTS and related genes. This is strong supportive evidence for a role of SCO4393 in aminosugar metabolism.

GLCNAC SENSING IS AFFECTED IN *S. COELICOLOR* SCO4393 MUTANTS

To create an *S. coelicolor* SCO4393 deletion mutant and a SCO4393-*nagB* double mutant, first gene replacement mutants were created whereby the SCO4393 gene from nucleotides 15 to 768 (relative to the transcriptional start site) was substituted with an apramycin resistance cassette. Homologous recombination of the gene was achieved by transformation with plasmid pGWS1052, which was constructed by cloning the resistance cassette between the upstream and downstream flanking regions of SCO4393 in the unstable multi-copy vector pWHM3. Correct recombination events were confirmed by resistance to apramycin and sensitivity to thiostrepton (for loss of the vector sequences) and by PCR. To create deletion mutants, the apramycin resistance cassette was excised from genome by Cre recombinase, expressed from the introduced pUWLcre plasmid, via the *loxP* sites located on either end of the cassette. Mutants were screened for sensitivity to apramycin and confirmed by PCR.

The *S. coelicolor* SCO4393 single mutant had a phenotype similar to its parent M145 on MM with GlcN and GlcNAc (Fig.2). Though both sugars induced antibiotic production and development on MM, development was impaired when GlcN was added. On R5 agar plates, production of the blue-pigmented actinorhodin was blocked or delayed in the mutant compared to the parental strain, and reduced in the presence of GlcN. Interestingly, GlcNAc sensing on R5 agar was lost in the SCO4393 mutant; the mutant developed abundant aerial hyphae and produced pigmented antibiotics in the presence of the aminosugar, in contrast to the parent. This suggests that SCO4393 affects the levels of an intermediate metabolite or metabolites required for the regulation of the GlcNAc response under rich growth conditions (feast).

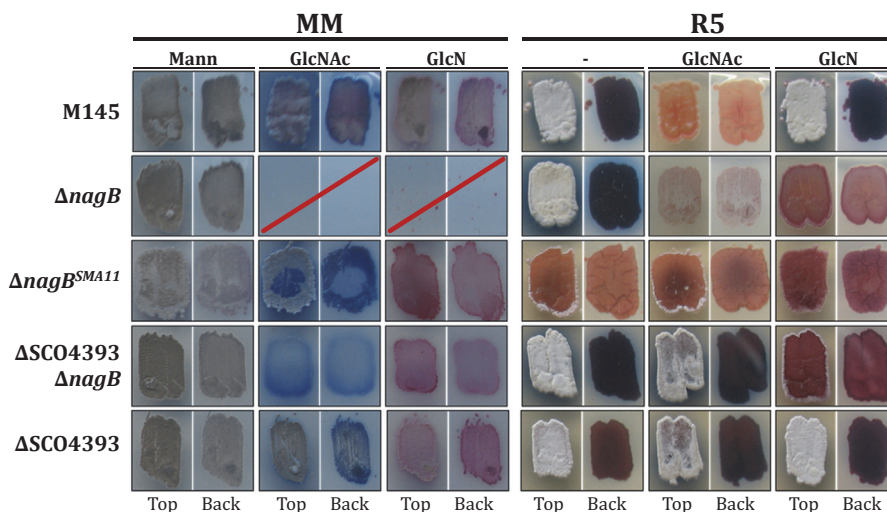


FIGURE 2. Phenotypic analysis of *S. coelicolor* SCO4393 mutants.

Spores of *S. coelicolor* M145, its *nagB* and SCO4393 deletion mutants, *nagB* suppressor mutant SMA11, and double mutants SCO4393-*nagB*, SCO4393-*nagA* and *nagA*-SCO4393 were plated onto minimal media (MM) or glucose-containing R5 agar plates, supplemented with 50 mM mannitol (Mann), glucosamine (GlcN) or *N*-acetylglucosamine (GlcNAc) as indicated. Mutants that failed to grow on GlcN or GlcNAc are indicated with a red line. The top view and bottom (back) view of the plates are indicated underneath.

Deletion of SCO4393 restored the ability of the *S. coelicolor nagB* mutant, which accumulates lethal levels of GlcN-6P or related metabolite(s), to grow on MM with GlcNAc and GlcN (Fig.2). The *nagB*-SCO4393 double mutant retained a phenotype similar to that of the parental strain and suppressor mutant SMA11 on MM with either aminosugar, though growth was less pronounced. The double mutant had a wild-type phenotype on R5 agar plates but failed to develop or produced blue-pigmented actinorhodin when GlcN was added, similar to *nagB* mutants. However, similarly as for the SCO4393 mutant, GlcNAc did not affect development or antibiotic production of the double mutant on R5 agar, suggesting that GlcNAc sensing had been lost. Thus, we present SCO4393 as a novel enzyme involved in aminosugar metabolism.

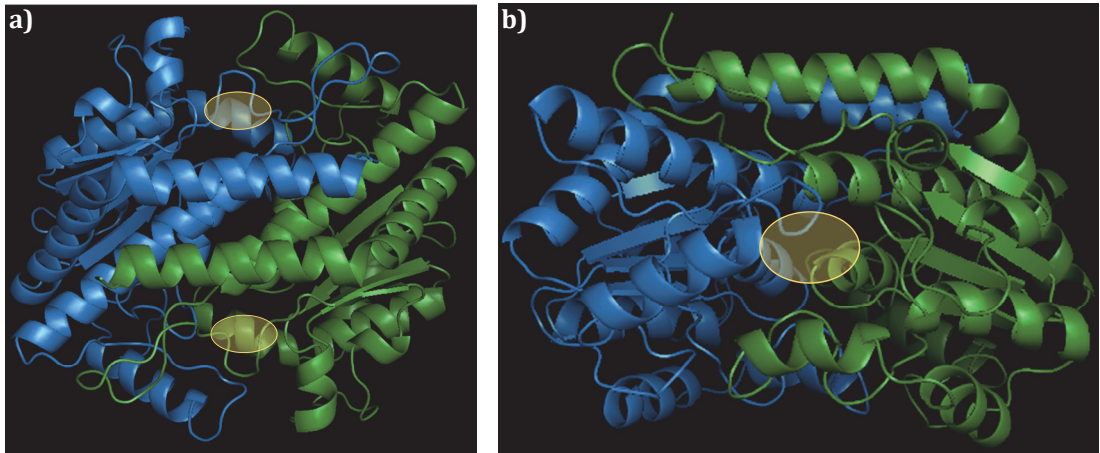


FIGURE 3. Crystal structure of SCO4393 dimer.

Image of the SCO4393 structure with determined by X-ray crystallography. The individual monomers (blue and green) of the dimer are shown with a view of both active sites (a), indicated in yellow, and a view into the active site (b), formed at the interface of the monomers.

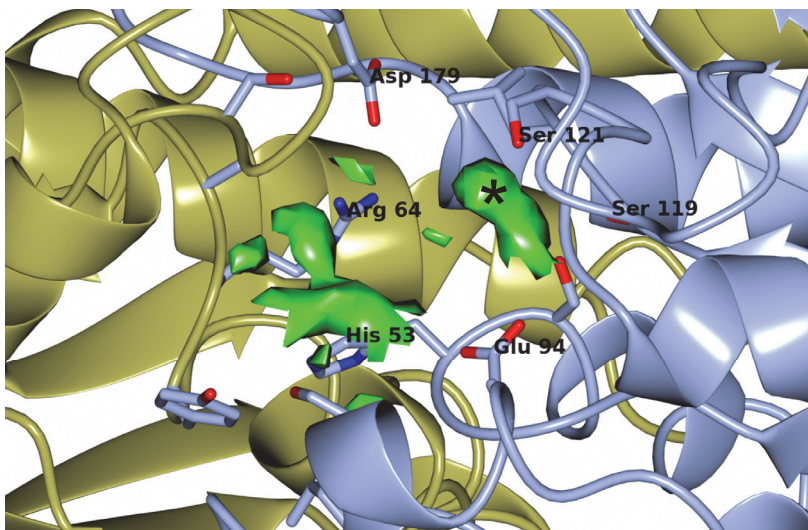


FIGURE 4. Trapped ligand intermediate in the active site of SCO4393.

Strong densities are shown in green within the active site of SCO4393. The density labelled with an asterisk (*) is proposed to be a phosphate group given its proximity and interactions with the serine residues. The monomers of SCO4393 shown in light blue and olive green.

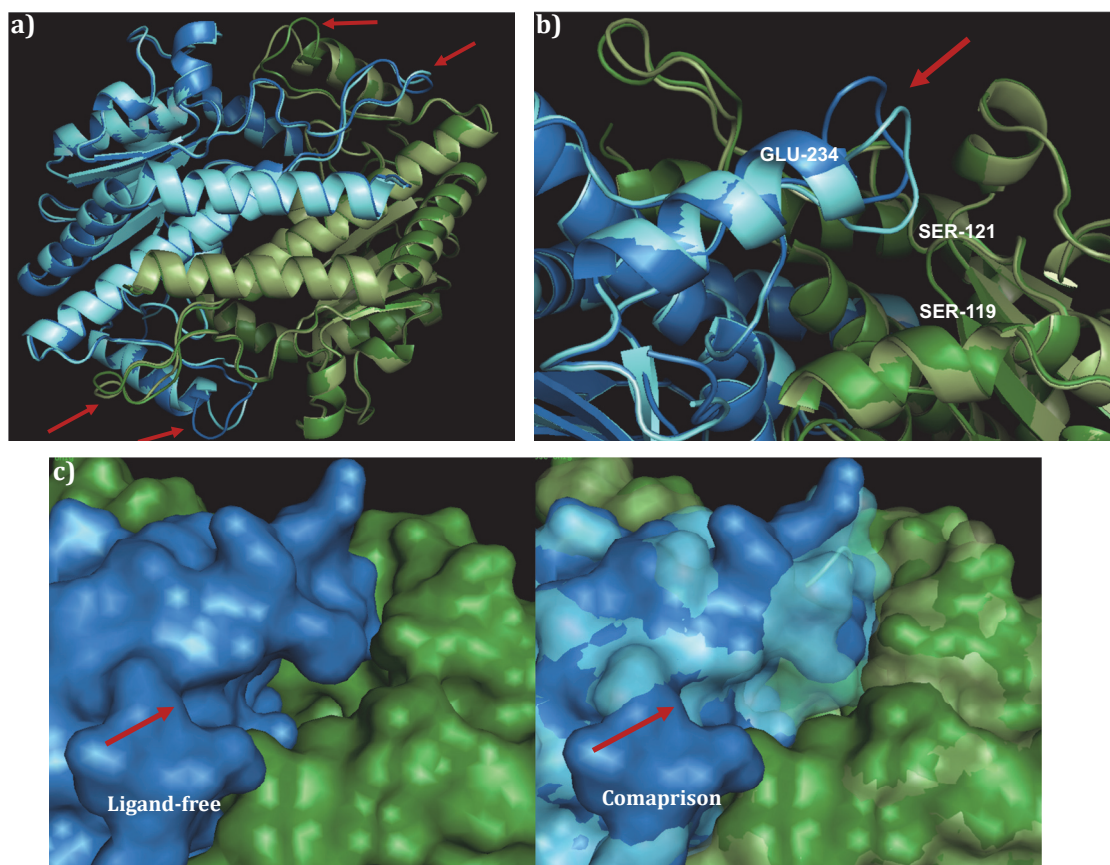


FIGURE 5. Comparison of SCO4393 with and without bound ligand.

Conformational shifts affecting access to the active site are indicated with red arrows. The subunits of ligand-bound SCO4393 are given in dark colours (blue and green) and the subunits of the ligand-free structure are given in light shades of blue and green.

- Global comparison of the ligand-free (light colours) and ligand-bound (dark colours) structure of SCO4393.
- Close up of conformational shift around the active site. Important residues relating to the position of the loop and for phosphate binding are labelled and the shift of the loop toward the active site is shown.
- Surface view of ligand-bound SCO4393 with open entry to the active site (dark colours) on the left and on the right, comparison with the ligand-free structure (light, transparent colours) with obscured entry. The surface view is in the same orientation as 5B.

STRUCTURAL INSIGHTS INTO SCO4393

N-terminally His₆-tagged SCO4393 was heterologously expressed in *E. coli* BL21 cells and purified to homogeneity (see Materials and Methods). The structure of SCO4393-His₆ was determined by X-ray crystallography. The refined 2.0 Å resolution model of SCO4393 consisted of residues 4-251 and positive electron density within the active site was noticed (described below). The refinement of the structure of the ligand-free enzyme, obtained by soaking the crystals in GlcN-6P, was determined to a resolution of 1.6 Å, using the 2.0 Å SCO4393 model as a template. *S. coelicolor* SCO4393 forms a dimer, with two active sites at the monomer interfaces on either side of the complex (Fig. 3). There is structural similarity between SCO4393 and other SIS-domain proteins, especially phosphoheptose isomerase BH3325 (3CVJ) of *Bacillus halodurans* and sedoheptulose-7-phosphate isomerase GmhA (2I2W), which is involved in lipopolysaccharide biosynthesis in *E. coli* (Taylor et al., 2008).

STRUCTURAL STUDIES OF SCO4393 LIGAND BINDING

Strong electron densities were observed within the SCO4393 active site, suggesting that the protein was isolated from *E. coli* with a bound ligand (Fig. 4). One density (labelled * in Fig. 4) is in close proximity to serine residues Ser54, Ser119 and Ser121, which have been implicated in phosphate binding. This suggests that the observed density relates to a phosphate group. Given the link to GlcNAc metabolism, the ligand could be GlcNAc-6P or a related phosphosugar. Interestingly, an Asp179Asn mutation is observed in suppressor mutants SMA11 and SMA13, which likely disrupts the catalytic activity of SCO4393 by destabilising the active site (Fig. 4), thus rendering it non-functional. Comparison of the structures of the substrate-free structure to that of the ligand-bound SCO4393 reveals minor changes in the structure of the protein with the exception of the conformational shifts of two loops (Fig. 5A). The loop formed between residues Ser226 and Glu234 is likely involved in keeping the ligand in position. In the substrate-free structure, the loops are shifted such that the binding pocket is largely obscured (Fig. 5B).

To investigate whether SCO4393 can bind GlcNAc-6P, crystals were soaked in 100 mM GlcNAc-6P for up to 5 min and the structures determined to a resolution of 2.5 Å. Crystals that had been soaked for less than five min retained an empty binding site. The active site of the crystal soaked for 5 min contained GlcNAc-6P but the enzyme was in ligand-free conformation, despite interactions with the *N*-acetyl-amine functional group and the phosphate moiety (Fig. 6). Indeed, the phosphate group was bound by the serine residues. However, the structure showed that GlcNAc-6P was in the alpha form, and NMR analysis of the ligand-soaking solution also determined it to be α -GlcNAc-6P (data not shown). Given that, to our knowledge, biological reactions of GlcNAc-6P require the β -form, we cannot rule out the consequences of soaking with α -GlcNAc-6P on binding and the potential enzymatic reaction.

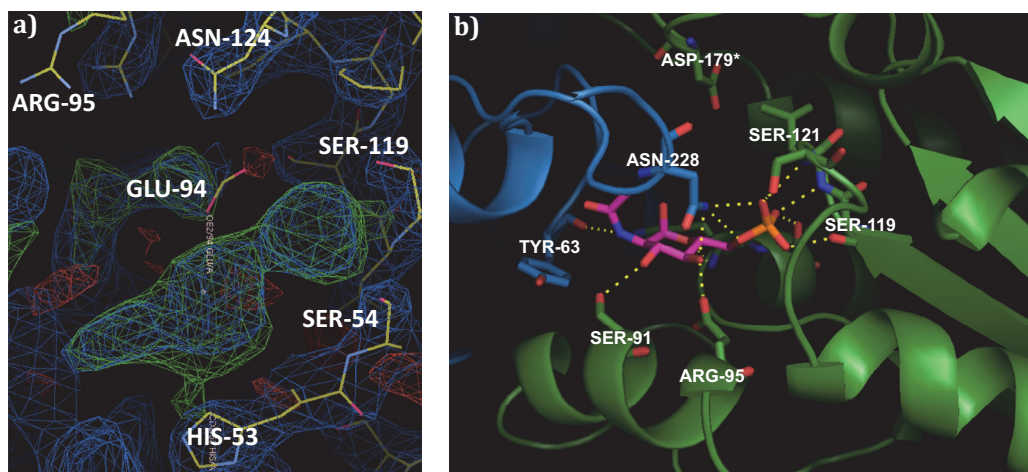


FIGURE 6. SCO4393 soak with GlcNAc-6P.

SCO4393 active site after soaking with 100 mM α -GlcNAc-6P for 5 minutes. SCO4393 remains in ligand-free conformation after soaking. The residues mutated in suppressor SMA11 (Asp179) is labelled by an *.

- View of the electron density of active site of SCO4393; mapped densities shown in dark blue, positive density differences in green and negative density differences in red. The large, positive density (green) in the centre shows the α -GlcNAc-6P with the phosphate group in the vicinity of the serine residues and the sugar moiety between GLU-94 and HIS-53.
- Close-up of the active site with the modelled GlcNAc-6P illustrating the interactions between the metabolite and residues of the SCO4393 active site. The subunits and residues of SCO4393 are shown in dark blue and green, GlcNAc-6P is shown in pink. Nitrogen is represented in blue, oxygen in red and phosphorus in orange.

SCO4393 LIGAND BINDING STUDIES

In addition to structural studies, SCO4393-ligand binding was also examined by isothermal titration calorimetry (ITC). Potential ligands were titrated at a concentration of 1 mM into 50 mM SCO4393 at 25°C. Of all the molecules tested, only α -GlcNAc-6P was bound by the protein, while no binding was seen for GlcNAc, GlcNAc-1P, Glc-6P or Fru-6P (Fig. 7). The importance of the *N*-acetyl group, given that GlcN-6P was unable to bind SCO4393, and the C6 phosphate group, given the complete lack of binding of GlcNAc and GlcNAc-1P, is highlighted.

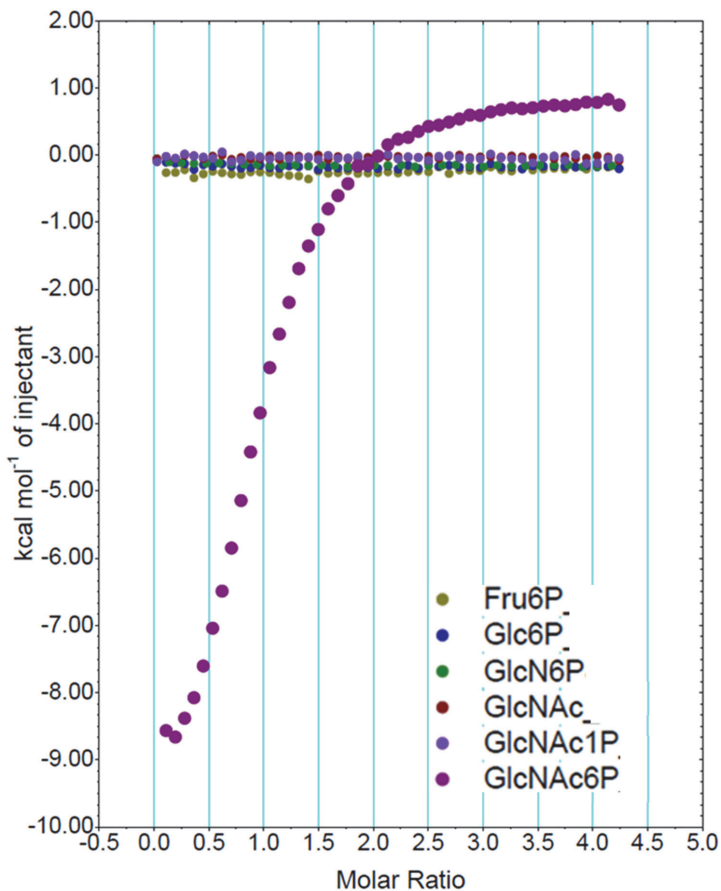


FIGURE 7. SCO4393 binding assays investigated by ITC.

For ITC binding studies, 1 mM ligand was titrated with 6 or 8 μ L injections into 50 mM purified SCO4393. Fru-6P (dark yellow), Glc-6P (blue), GlcN-6P (green), GlcNAc (dark red), GlcNAc-1P (bright purple) and α -GlcNAc-6P (aubergine) were tested. Note that SCO4393 was only able to bind α -GlcNAc-6P.

DISCUSSION

N-acetylglucosamine is a preferred carbon source for streptomycetes and stands at the cross-roads between aminosugar metabolism, glycolysis and cell-wall synthesis (Fig. 8). The molecule also plays a key role in nutrient sensing and the ultimate decision to initiate development and antibiotic production (Rigali *et al.*, 2008). Deletion of *nagA* or *nagB* results in altered antibiotic production, likely due to the accumulation of GlcNAc-6P or GlcN-6P, when grown in the presence of GlcNAc or GlcN, respectively (Świątek *et al.*, 2012a). This prompted further investigation into the possibility of altering the flux of GlcN(Ac) as a strategy to activate antibiotic production. In this work, we investigated a new enzyme involved in aminosugar metabolism that was discovered via a suppressor screen of *nagB* mutants, which fail to grow on GlcN or GlcNAc. Suppressor mutations that relieved aminosugar sensitivity of *nagB* mutants were found in SCO4393, which encodes a likely phosphosugar isomerase (Świątek, 2012).

The genetic environment around SCO4393 is highly conserved in streptomycetes. Homologs of SCO4393, with relatively low sequence similarity (around 30%), are also found in bacteria such as firmicutes and proteobacteria and in these bacteria, the gene is often found associated with *pts* transporter genes or adjacent to *nagA* and *glmS*. Both NagA and GlmS generate GlcN-6P, from GlcNAc-6P and Fru-6P, respectively (Fig. 8). Interestingly, divergently expressed from SCO4393 is the gene of iron-homeostasis regulator DmdR1 (SCO4394) in *S. coelicolor*, which is induced by GlcNAc (Craig *et al.*, 2012). Addition of iron to rich media with GlcNAc restores antibiotic production and development under feast conditions in *S. coelicolor* (Lambert *et al.*, 2014). These data suggest linkage between GlcNAc and iron homeostasis in *Streptomyces*.

The crystal structure of SCO4393 was resolved to a high resolution and showed that the entry of the SCO4393 active site is blocked in the substrate-free conformation, while it is opening the ligand-bound form. The ligand-bound structure showed densities of an unknown ligand trapped in the active site. Given the proximity of the observed densities to the serine residues, which are most likely involved in phosphate binding, we speculate that part of the observed density is that of the phosphate group of the ligand, kept in place by Ser54, Ser119 and Ser121. Indeed, the serine residues of SCO4393 bound the phosphate group of GlcNAc-6P (Fig. 6), after crystals were soaked in the compound. ITC binding studies demonstrated that SCO4393 binds α -GlcNAc-6P, while it failed to bind GlcNAc, GlcNAc-1P, Glc-6P or Fru-6P (Fig. 7). Though this suggests that the phosphate group and acetyl group may be essential, proteins from the crystal soaked in α -GlcNAc-6P for 5 min remained in ligand-free form, despite the interactions of the SCO4393 backbone with both the phosphate and acetyl groups of the ligand. The potential catalytic residues of the SCO4393 binding pocket are characteristic of sugar isomerases, such as glucose-6P isomerase (Solomons *et al.*, 2004), with His, Arg and Glu involved in the opening and closing of the ring, and stabilization of the intermediate. Preliminary modelling of GlcNAc-6P onto the density within the active site of ligand-bound SCO4393 suggests that the metabolite would have to be in an open-ring conformation, with the further density being an acetyl-amine group (NH-C=O-CH₃) (Fig. 4). It should be noted that experiments were performed with α -GlcNAc-6P, while β -GlcNAc-6P is thought to be biologically favoured. Taken together, the *in vitro* data suggest that the substrate is a phospho-aminosugar, and related to GlcNAc-6P.

The key question to address is, what is the toxic molecule that accumulates in *nagB* mutants grown on high concentrations of GlcN or GlcNAc? Mutants that lack a functional NagA enzyme accumulate high levels of GlcNAc-6P, which is lethal in *B. subtilis* and *E. coli* (Plumbridge, 2015). However, *S. coelicolor nagA* null mutants grow in the presence of

GlcNAc, strongly suggesting that toxicity is not caused by GlcNAc-6P or direct metabolic derivatives, and that instead the toxic compound is derived from GlcN-6P. Indeed, deletion of *nagA* is sufficient to restore growth of *nagB* mutants on aminosugars, even though preliminary metabolomic experiments revealed strong accumulation of GlcNAc-6P in these mutants (MU, GPvW and Christoph Müller, unpublished data). Zooming in on GlcN-6P, this is the starter molecule for cell-wall biosynthesis. We believe that the biosynthetic pathway of Lipid II may indeed play a major role in toxicity. For one, toxicity of GlcN(Ac) is relieved when cells are pre-grown to early exponential phase (Świątek *et al.*, 2012a). At this stage, peptidoglycan biosynthesis is maximal, and precursors are readily incorporated. This may not yet be the case for germinating spores. A second indication that cell-wall precursors play a role in toxicity comes from so-called L-forms. These are cells that lack a wall, enforced by growth in the presence of the cell-wall targeting antibiotic penicillin and the cell wall hydrolase lysozyme (Errington, 2013; Mercier *et al.*, 2014). Streptomycetes can also be forced to produce L-forms (Innes & Allan, 2001), and these sustain spontaneous mutations in the *mur* genes that encode components of the cell-wall precursor pathway. This again suggests that accumulation of cell-wall precursors may be lethal for streptomycetes. Metabolic analysis of SCO4393 suppressor mutants showed that they accumulate GlcN-6P (preliminary data, not shown), which would suggest that the absence of SCO4393 renders GlcN-6P accumulation non-toxic and that SCO4393 does not block GlcN-6P production but rather acts on GlcN-6P or its derivative.

Taken together, our data suggest that one or more toxic intermediates are derived from GlcN-6P but not from GlcNAc-6P, and that they relate to cell-wall precursor biosynthesis. SCO4393 is likely directly involved in the accumulation of the toxic intermediate. Structural studies indicate that SCO4393 binds a phospho-aminosugar in its linear form, structurally related to GlcNAc-6P. The latter is supported by ITC experiments that revealed that SCO4393 binds α -GlcNAc-6P. However, this is in direct conflict with the biological experiments that show that accumulation of GlcNAc-6P in cells expressing SCO4393 does not affect growth of *S. coelicolor*. Hence, we propose that the substrate of SCO4393 is a related aminosugar, with *N*-acetylgalactosamine-6P and *N*-acetylglutamate-6P as candidates, whereby *N*-acetylgalactosamine-6P is a GlcNAc-6P isomer and precursor for bacterial cell-wall components. We are currently focusing our research on elucidating the precise reaction that is catalysed by SCO4393 and the nature of the toxic intermediate.

ACKNOWLEDGEMENTS

We are grateful to Marcellus Ubbink and Vera van Noort for stimulating discussions, and to Raffaella Tassoni for help with the ITC experiments.